

RESEARCH AND EDUCATION

Accuracy of capturing oncology facial defects with multimodal image fusion versus laser scanning



Rachael Y. Jablonski, BDS, MFDS RCS (Edin),^a Cecilie A. Osnes, BA (Hons), MSc,^b
Balvinder S. Khambay, BDS, PhD, FDS RCS(Eng), MOrth RCS(Edin), FDS(Ortho) RCS(Eng),^c
Brian R. Nattress, BChD, PhD, FDS RCS(Edin), MRD RCS(Edin), FDTFEd,^d and
Andrew J. Keeling, BSc, BDS, MFGDP, PhD^e

Fabrication of conventional facial prostheses is a labor-intensive process comprising multiple clinical and laboratory stages.¹ These include obtaining a facial moulage that records the defect, surrounding facial features, and the unaffected side for unilateral defects.¹ Inaccuracies during impression making can occur because of soft-tissue compression, the patient's reflex movements, or by the lack of support for the impression material.² After obtaining the facial moulage, a gypsum cast is poured, and a wax pattern of the prosthesis is produced. A negative mold is then fabricated and used to produce the silicone prosthesis.¹ Achieving a satisfactory prosthesis that will mask the missing facial tissue is highly dependent on the skills of the maxillofacial prosthodontist.³

ABSTRACT

Statement of problem. Fabrication of conventional facial prostheses is a labor-intensive process which traditionally requires an impression of the facial defect and surrounding tissues. Inaccuracies occur during the facial moulage because of soft-tissue compression, the patient's reflex movements, or the lack of support for the impression material. A variety of 3D imaging techniques have been introduced during the production of facial prostheses. However, the accuracy of the different imaging techniques has not been evaluated sufficiently in this clinical context.

Purpose. The purpose of this in vitro study was to compare the difference in accuracy of capturing oncology facial defects with multimodal image fusion and laser scanning against a cone beam computed tomography (CBCT) reference scan.

Material and methods. Ten gypsum casts of oncology facial defects were acquired. To produce reference models, a 3D volumetric scan was obtained using a CBCT scanner and converted into surface data using open-source medical segmentation software. This model was cropped to produce a CBCT mask using an open-source system for editing meshes. The multimodal image fusion model was created using stereophotogrammetry to capture the external facial features and a custom optical structured light scanner to record the defect. The gypsum casts were also scanned using a commercial 3D laser scanner to create the laser-scanned model. Analysis of the best fit of each experimental model to the CBCT mask was performed in MeshLab. The unsigned mean distance was used to measure the absolute deviation of each model from the CBCT mask. A paired-samples *t* test was conducted to compare the mean global deviation of the 2 imaging modalities from the CBCT masks ($\alpha=.05$).

Results. A statistically significant difference was found in the mean global deviation between the multimodal imaging model ($220 \pm 50 \mu\text{m}$) and the laser-scanned model ($170 \pm 70 \mu\text{m}$); ($t(9)=2.56$, $P=.031$). The color error maps illustrated that the greatest error was located at sites distant to the prosthesis margins.

Conclusions. The laser-scanned models were more accurate; however, the mean difference of $50 \mu\text{m}$ is unlikely to be clinically significant. The laser scanner had limited viewing angles and a longer scan time which may limit its transferability to maxillofacial practice. (J Prosthet Dent 2019;122:333-8)

This study is supported by the Royal College of Surgeons of Edinburgh (grant number: SRG/16/094). The funding source had no influence in conducting the study, writing of the report, or the decision to submit the manuscript for publication.

^aAcademic Clinical Fellow and Specialty Registrar, Department of Restorative Dentistry, School of Dentistry, University of Leeds, Leeds, United Kingdom.

^bResearch Assistant, Department of Restorative Dentistry, School of Dentistry, University of Leeds, Leeds, United Kingdom.

^cProfessor, Institute of Clinical Sciences, College of Medical and Dental Sciences, The School of Dentistry, University of Birmingham, Birmingham, United Kingdom.

^dSenior Lecturer and Honorary Consultant, Department of Restorative Dentistry, School of Dentistry, University of Leeds, Leeds, United Kingdom.

^eClinical Associate Professor, Department of Restorative Dentistry, School of Dentistry, University of Leeds, Leeds, United Kingdom.

Clinical Implications

The multimodal image fusion technique shows potential as a true and precise method of capturing oncology facial defects based on previous *in vitro* research and compares well with a commercially available laser scanner. The approach combines the initial short capture time of stereophotogrammetry with the ability of the structured light scanner to process deeper defects. This makes the multimodal imaging technique a practical option to use in the clinical environment, and further research is planned to appraise its clinical use.

Three-dimensional imaging and computer-aided design and computer-aided manufacturing (CAD-CAM) technologies are becoming more commonplace in the hospital setting and have many applications in dentistry and oral and maxillofacial surgery.⁴ A variety of 3D-imaging techniques have been introduced for the production of facial prostheses in an attempt to overcome some of the limitations of conventional impressions. Potential benefits include improved patient comfort, reduced invasiveness, and efficiency of data collection.^{2,5} CAD processes may also reduce dependence on the artistic skills of the maxillofacial prosthetist.⁶ In addition, application of CAM processes could significantly reduce the time taken and number of clinical stages for facial prosthesis production.¹

Data from medical computed tomography imaging systems have been successfully used in the production of facial prostheses, for example, during the manufacture of orbital or nasal prostheses.^{7,8} Potential limitations in using 3D models derived from computed tomography data include the need for volume rendering to obtain a 3D representation of the anatomical structures.⁶ This process can be influenced by various factors leading to a change in dimensions when compared with the original anatomy.⁹ In addition, there may be concerns associated with exposure to radiation and the cost of resources for manipulating large volumes of data.^{1,6}

Noninvasive systems such as stereophotogrammetry can produce a 3D surface model from multiple viewpoints in a synchronized manner with a short capture time and clinically acceptable accuracy.¹⁰ The successful use of stereophotogrammetry to produce facial prostheses on superficial defects has been reported.¹ However, this imaging modality makes it difficult to record deep defects because the baseline separation of the cameras does not usually permit binocular vision in such regions. Optical scanning to supplement the missing data from the deeper defect area based on a multimodal imaging technique has been suggested to overcome this limitation.¹¹

Laser surface scanning is an alternative technique to stereophotogrammetry and has been successfully introduced into the workflow for producing facial prostheses.^{6,12} As with stereophotogrammetry, laser scanning of deeper regions and undercuts is limited by the separation of the laser-line generator and the receptor camera.⁶ In addition, some systems will require the patient to remain motionless for a prolonged time which could further limit data acquisition.¹

Digital data acquisition and rapid prototyping have the potential to assist the manufacturing process in a variety of ways. First, stereolithic models of the defect can be produced, duplicated, and used by the maxillofacial prosthetist to produce a wax pattern of the prosthesis in the usual way.¹⁰ Second, positive replicas of the actual prostheses can be created in wax, evaluated on the patient, and processed through flasking and investment.¹³ In addition, negative molds for casting the prosthesis can be produced, which would eliminate the need for conventional flasking and investment procedures.^{6,14} More recently, 3D color printing and infiltration with medical-grade silicone have been reported.¹⁵

Despite the many clinical reports exploring the use of 3D-imaging and CAD-CAM technologies in the production of facial prostheses, there has been little evaluation of the accuracy of different imaging techniques for maxillofacial prosthetics. Therefore, the purpose of this *in vitro* study was to compare the difference in accuracy between multimodal image fusion (stereophotogrammetry plus structured light optical scanning) and laser scanning, for capturing oncology facial defects, against a cone beam computed tomography (CBCT)-scanned model. A CBCT scan was selected as the reference scan because of the accuracy and reliability of its measurements.¹⁶ The null hypothesis was that there was no statistically significant difference in the unsigned mean global deviation between the multimodal imaging models, laser-scanned models, and reference CBCT scan.

MATERIAL AND METHODS

Ethical approval was obtained, and a sample of 10 existing gypsum casts of various oncology facial defects was acquired from the maxillofacial laboratories within the Leeds Teaching Hospitals and Bradford Teaching Hospitals. To the best of the authors' knowledge, the difference in accuracy deemed to be clinically important in this context has not yet been formally defined. Therefore, the sample size for this pilot study was determined by the number of relevant gypsum casts available within the units. The sample included 4 nasal defects, 5 orbital defects, and 1 combined defect. Images of the meshes obtained of the sample have been included in a previous article.¹¹



Figure 1. Stereophotogrammetry (DI3D; Dimensional Imaging Ltd) used to capture external facial features during multimodal imaging technique.

A 3D volumetric scan of each cast was made using a CBCT scanner (NewTomVG; Cefla SC). This was converted into surface data using an open-source medical segmentation software program (ITK-SNAP; <http://www.itksnap.org>), and the data were cropped to produce a CBCT mask using an open-source system for editing meshes (MeshLab; <http://www.meshlab.net>). The CBCT masks formed the reference scan for comparing the other imaging modalities.

Three-dimensional models were produced for each cast using multimodal image fusion with the method as reported in a previous article.¹¹ Before scanning the gypsum casts, the stereophotogrammetry and optical structured light scanner were calibrated with calibration targets. The external facial features were then captured using stereophotogrammetry (DI3D; Dimensional Imaging Ltd) (Fig. 1). This obtained 4 photographs of the gypsum cast in a synchronized manner. The 2 stereo pairs of images were then processed using a passive stereophotogrammetry software program to generate a 3D surface image. The defect was then independently imaged using a custom optical structured light scanner—comprising 2 commercially available cameras (IDS uEye LE monochrome 1MP cameras; IDS Imaging Development Systems GmbH) and a digital light-processing projector (Optoma PK201; Optoma Europe Ltd) (Fig. 2). Depending on the complexity of the defect, up to 10 images were made using the custom optical structured light scanner. The models were aligned, merged, and resurfaced using MeshLab to produce a single fused model of the external facial features and defect. In the previous study, the precision (intraoperator repeatability) of the multimodal image fusion technique was also evaluated by repeating the process of aligning the model of the defect to the external facial features.¹¹

Each gypsum cast was captured using a commercial 3D laser scanner (3D Scanner Ultra HD; NextEngine, Inc)



Figure 2. Custom optical structured light scanner used to capture defect during multimodal imaging technique. Scanner comprised 2 commercially available cameras each measuring 34×32×41.3 mm (IDS uEye LE monochrome 1MP cameras; IDS Imaging Development Systems GmbH) and digital light-processing projector of similar size to smartphone (Optoma PK201; Optoma Europe Ltd).

(Fig. 3). The scanner was calibrated with the manufacturer's reference object before scanning the casts. Alignment marks were made on each cast in accordance with the manufacturer's instructions. The autodrive along with the bracket scanning setting were used to enable the cast to be scanned in 3 consecutive angles. Where there were visible areas of data missing from the 3D model (for example, due to the presence of competing undercuts), the cast was repositioned on the autodrive at up to 3 different inclinations and a new scan was obtained. Each individual mesh was aligned using alignment pins, trimmed to remove unwanted data, and then fused using a software program (ScanStudio; NextEngine, Inc) to produce a single fused model comprising surface data.

Analysis of the best fit of each experimental model to the CBCT mask was performed in MeshLab. The multimodal image fusion model and laser-scanned model were independently aligned to the CBCT mask based on the iterative closest-point algorithm.¹⁷ The unsigned mean distance between all the 3D points of the experimental model and CBCT mask was used to calculate the global absolute deviation of each model from the CBCT mask. This was necessary because after alignment, some parts of the experimental model were behind the CBCT mask, whereas other parts were in front of it, resulting in both positive and negative distance values. The unsigned mean distance prevented the positive and negative distance values from canceling each other out and underestimating the magnitude of the difference.¹⁸ Color error maps were also produced for each CBCT mask to identify data points on both experimental models which deviated from the CBCT mask under different distance parameters.



Figure 3. Commercial 3D laser scanner used to produce laser-scanned models (3D Scanner Ultra HD; NextEngine, Inc).

The 3D models for 2 of the gypsum casts had missing data because of extreme undercuts. As the subsequent prostheses would not extend into this area, the corresponding casts were marked by a maxillofacial prosthetist to identify the clinically relevant areas. The unsigned mean distance was reassessed excluding those data points within the defect border which lay several millimeters from the clinically relevant area. A paired-samples *t* test was conducted to compare the overall unsigned mean global deviation of the 2 imaging modalities from the CBCT masks ($\alpha=.05$).

RESULTS

The unsigned mean global absolute deviation of the imaging modalities from the CBCT masks are outlined in Table 1. A statistically significant difference was found in the unsigned mean global deviation between the multimodal imaging models ($220 \pm 50 \mu\text{m}$) and laser-scanned models ($170 \pm 70 \mu\text{m}$) ($t(9)=2.56$, $P=.031$).

Color error maps were produced for each CBCT mask to demonstrate points on each model, which were within different parameters for unsigned distance (Fig. 4). The color error maps for the multimodal image fusion models illustrated that the greatest error was located at sites distant to the prosthesis margins (for example, within the base of the defect or along the facial contours). In comparison, the laser-scanned models appeared to have a generalized reduction in the greatest error category ($>500 \mu\text{m}$) compared with the multimodal image fusion models. A few laser-scanned models had more holes within the mesh because of the limited viewing angles.

DISCUSSION

The results of the present study support rejection of the null hypothesis. Both the multimodal imaging models and laser-scanned models had a mean global absolute

Table 1. Global deviation (μm) of imaging modalities from CBCT mask

Cast	Average Global Deviation \pm Standard Deviation (μm)	
	Multimodal Image Fusion*	Laser Scanning
A	140 \pm 130	90 \pm 80
B	150 \pm 130	120 \pm 150
C	190 \pm 150	150 \pm 130
D	210 \pm 210	150 \pm 250
E	230 \pm 260	230 \pm 280
F	230 \pm 230	180 \pm 330
G	250 \pm 320	320 \pm 810
H	250 \pm 210	170 \pm 310
I	260 \pm 200	150 \pm 180
J	310 \pm 290	120 \pm 170
Overall	220 \pm 50	170 \pm 70

CBCT, cone beam computed tomography. *Jablonski et al.¹¹

deviation of under $250 \mu\text{m}$ from the CBCT masks. Although thresholds for clinically relevant differences in accuracy have not been formally defined in this context, the authors suggest that a mean global absolute deviation of less than $250 \mu\text{m}$ is likely to be clinically acceptable. The laser scanner produced 3D models that deviated to a statistically significant lesser degree from the reference CBCT scan than the multimodal image fusion models. The overall difference in the mean global deviation between the imaging modalities was $50 \mu\text{m}$. Although statistically significant, the difference between the 2 modalities is unlikely to be clinically significant with respect to the fit of the prostheses as the color error maps showed that the greatest error was usually located at sites distant from the prosthesis margins. However, the location of these distant errors could impair the prostheses design, for example, unilateral defects where the position of the orbit needs to be carefully reproduced.

One of the difficulties in the present study was selecting an appropriate model to use as a reference standard. As previously discussed, there are potential limitations in using 3D models derived from CBCT data. Volume rendering, which is performed to produce a 3D representation of the object, can be influenced by a variety of factors including the isovalue used to extract the surface. This could change the anatomical dimensions in actual patients; however, it is unlikely to have a major impact in this study as gypsum casts are of uniform density. Furthermore, the CBCT scan had a voxel size of $300 \mu\text{m}$ and therefore may lose fine details, consequently decreasing its precision in small volumes. In addition, the alignment process itself is likely to introduce a degree of error because of the nature of the iterative closest-point algorithm.¹⁷

The laser scanner was able to capture fine details and produced models that more accurately matched the CBCT models. Only cast G demonstrated a greater mean global absolute deviation with the laser scanner than with the multimodal image fusion technique. This cast had extreme

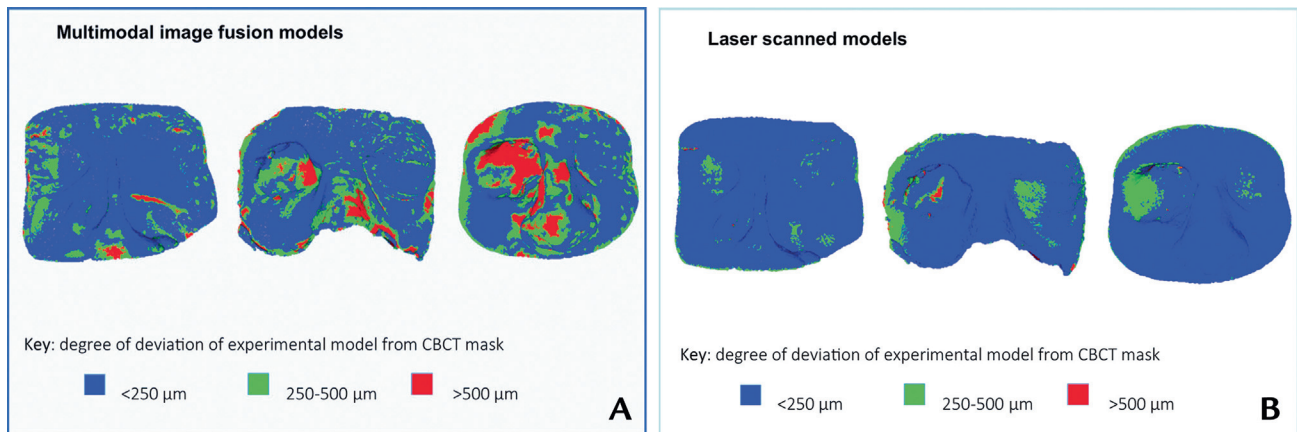


Figure 4. Representative color error maps (left=cast A, middle=cast F, right=cast J). A, Multimodal image fusion models: note greater error category (red) generally located at sites distant to prosthesis margins. B, Laser-scanned models: note generalized reduction in greater error category (red) compared with multimodal image fusion models. CBCT, cone beam computed tomography.

undercuts that had been poorly captured by the laser scanner, resulting in a much higher maximum deviation value and consequently a greater mean global absolute deviation. This relates to one of the limitations of the laser scanner which is the limited viewing angles (because of the size of the stereo baseline), which meant that some areas of undercut were poorly captured resulting in holes within the model. Each cast was therefore repositioned and scanned up to 3 times at different inclinations to maximize data acquisition. Stitching together multiple scans in this manner has the potential to introduce errors within the final model.¹⁷ In addition, each scan took several minutes to complete based on the manufacturer's recommended settings. This may limit the scanner's applications in the clinical environment as patients may not be able to remain motionless for this prolonged time.

The method of multimodal image fusion has previously been shown to have potential as a true and precise method of capturing facial defects based on *in vitro* data.¹¹ This approach combines the initial short capture time of stereophotogrammetry with the ability of the structured light scanner to capture the internal surfaces of the defect. Although multimodal image fusion had a greater mean global absolute deviation than the laser scanner, this appeared to be within clinically acceptable limits. The stereophotogrammetry software had some difficulties in aligning the left and right pairs of scans in this study, presumably because of indistinct features on the gypsum cast compared with the characteristics of actual facial tissues. Therefore, this source of error may be reduced in the clinical environment.

The time necessary for multimodal image fusion included both the initial data-acquisition time and the postprocessing time. Data acquisition first involved stereophotogrammetry to capture the external facial features, and this has the efficiency of a single photographic exposure. The custom structured light scanner

then captured the internal surfaces of the defect and required approximately 1 second per 3D image (up to 10 images were made depending on the complexity of the defect). Postprocessing alignment and surfacing were performed using an open-source software program for editing meshes (MeshLab; <http://www.meshlab.net>). The postprocessing time would be dependent on the operator's experience whereby an experienced user could align and surface a set of scans in a few minutes, whereas an inexperienced user may take up to 30 minutes. Recent improvements in automatic registration would be a useful addition, and freely available source codes can be downloaded in this regard; however, this was not used in the present study.¹⁹

The short acquisition time and recent improvements in automatic registration may make multimodal image fusion a more practical clinical solution. The laser scanner had a prolonged scan time, and although accurate and useful for comparison in this study, its clinical application would be limited. The custom structured light scanner used in this study required a laptop and Universal Serial Bus cable connection. A scanner with a wireless connection may be better suited for clinical applications. Commercial scanners (for example, Artec Space Spider; Artec 3D) are available with a similar field of view and reported resolution, which are fully ergonomic and run at 7.5 frames per second.

For analysis, deviation was assessed across the entire surface of the CBCT mask, and therefore, the results could have underestimated errors at clinically important areas such as the prosthesis margins.¹¹ However, it was also important to not only capture the defect but also obtain sufficient accurate data from the surrounding facial features so that the contours of a prosthesis could be made in harmony with the surrounding tissues. The color error maps did indicate that this was not the case as the greatest error was usually located away from clinically

important areas. A complete set of color error maps are available, enabling a judgment to be made regarding the clinical relevance of the error patterns (<https://medhealth.leeds.ac.uk/info/1240/research>). An alternative approach could have been to perform a regional analysis on the most clinically important areas, and this is a potential consideration for future studies.¹⁸ Further research is also planned to evaluate what difference in accuracy would be clinically important in this context and to determine what factors would impact prosthesis fit such as error location.

There are limitations relating to the in vitro nature of this study. The gypsum casts had artificially trimmed edges and smooth featureless surfaces and were produced using the type III yellow stone. These factors may have impeded precise alignment with any of the different imaging modalities. Further research is therefore needed to evaluate their performance in the clinical environment.

CONCLUSIONS

Based on the findings of this in vitro study, the following conclusions were drawn:

1. Both the laser scanner and the multimodal imaging technique captured the defect and external facial features to an acceptable level of accuracy.
2. Although the laser scanner had a statistically significant lower mean global deviation than the multimodal imaging method, the mean difference of 50 μm is unlikely to have a clinical impact.
3. The short capture time and ability to process into deeper defects make the multimodal imaging technique a more practical option for the clinical environment.

REFERENCES

1. Liacouras P, Garnes J, Roman N, Petrich A, Grant GT. Designing and manufacturing an auricular prosthesis using computed tomography, 3-dimensional photographic imaging, and additive manufacturing: a clinical report. *J Prosthet Dent* 2011;105:78-82.
2. Runte C, Dirksen D, Delere H, Thomas C, Runte B, Meyer U, et al. Optical data acquisition for computer-assisted design of facial prostheses. *Int J Prosthodont* 2002;15:129-32.
3. Sun J, Zhang FQ. The application of rapid prototyping in prosthodontics. *J Prosthodont* 2012;21:641-4.
4. Dawood A, Marti B, Sauret-Jackson V, Darwood A. 3D printing in dentistry. *Br Dent J* 2015;219:521-9.

5. Tsuji M, Noguchi N, Ihara K, Yamashita Y, Shikimori M, Goto M. Fabrication of a maxillofacial prosthesis using a computer-aided design and manufacturing system. *J Prosthodont* 2004;13:179-83.
6. Cheah CM, Chua CK, Tan KH, Teo CK. Integration of laser surface digitizing with CAD/CAM techniques for developing facial prostheses. Part 1: design and fabrication of prosthesis replicas. *Int J Prosthodont* 2003;16:435-41.
7. Li S, Xiao C, Duan L, Fang C, Huang Y, Wang L. CT image-based computer-aided system for orbital prosthesis rehabilitation. *Med Biol Eng Comput* 2015;53:943-50.
8. Neto R, Costa-Ferreira A, Leal N, Machado M, Reis A. An engineering-based approach for design and fabrication of a customized nasal prosthesis. *Prosthet Orthot Int* 2015;39:422-8.
9. Ferraz EG, Andrade LC, dos Santos AR, Torregrossa VR, Rubira-Bullen IR, Sarmiento VA. Application of two segmentation protocols during the processing of virtual images in rapid prototyping: ex vivo study with human dry mandibles. *Clin Oral Investig* 2013;17:2113-8.
10. Sabol JV, Grant GT, Liacouras P, Rouse S. Digital image capture and rapid prototyping of the maxillofacial defect. *J Prosthodont* 2011;20:310-4.
11. Jablonski RY, Osnes CA, Khambay BS, Nattress BR, Keeling AJ. An in-vitro study to assess the feasibility, validity and precision of capturing oncology facial defects with multimodal image fusion. *Surgeon* 2018;16:265-70.
12. Ciocca L, Mingucci R, Gassino G, Scotti R. CAD/CAM ear model and virtual construction of the mold. *J Prosthet Dent* 2007;98:339-43.
13. Feng Z, Dong Y, Zhao Y, Bai S, Zhou B, Bi Y, et al. Computer-assisted technique for the design and manufacture of realistic facial prostheses. *Br J Oral Maxillofac Surg* 2010;48:105-9.
14. Ciocca L, Bacci G, Mingucci R, Scotti R. CAD-CAM construction of a provisional nasal prosthesis after ablative tumour surgery of the nose: a pilot case report. *Eur J Cancer Care (Engl)* 2009;18:97-101.
15. Xiao K, Wuergler S, Mostafa F, Sohaib A, Yates JM. Colour image reproduction for 3D printing facial prostheses. In: Shishkovsky I, editor. *New trends in 3D printing*. 2016, doi: 10.5772/63339. Available at: <https://www.intechopen.com/books/new-trends-in-3d-printing/colour-image-reproduction-for-3d-printing-facial-prostheses>. Accessed October 3, 2018.
16. El-Beialy AR, Fayed MS, El-Bialy AM, Mostafa YA. Accuracy and reliability of cone-beam computed tomography measurements: influence of head orientation. *Am J Orthod Dentofacial Orthop* 2011;140:157-65.
17. Besl PJ, McKay ND. A method for registration of 3-D shapes. *IEEE Trans Pattern Anal Mach Intell* 1992;14:239-56.
18. Khambay B, Ullah R. Current methods of assessing the accuracy of three-dimensional soft tissue facial predictions: technical and clinical considerations. *Int J Oral Maxillofac Surg* 2015;44:132-8.
19. Zhou Q-Y, Park J, Koltun V. Fast global registration. In: Leibe B, Matas J, Sebe N, Welling M, editors. *Computer vision – ECCV 2016 14th European conference proceedings part II*. Cham: Springer International Publishing; 2016. p. 766-82.

Corresponding author:

Dr Rachael Y. Jablonski
Leeds School of Dentistry
Clarendon Way
University of Leeds
Leeds LS2 9LU
UNITED KINGDOM
Email: rachaeljablonski@gmail.com

Acknowledgments

The authors would like to thank Tim Zoltie, Paul Bartlett, and Richard Hardcastle for their ongoing support during the project.

Copyright © 2019 by the Editorial Council for *The Journal of Prosthetic Dentistry*.
<https://doi.org/10.1016/j.prosdent.2018.10.017>